Hyperspherical close-coupling calculations for helium in a strong magnetic field

M. Braun
Physics Department, University of South Africa, P.O. Box 392, 0003 Pretoria, South Africa

W. Schweizer* and H. Elster
Institut for Astronomie und Astrophysik, Abteilung Theoretische Astrophysik, Universität Tübingen, Auf der Morgenstelle 10, D-72076 Tübingen, Germany

(Received 10 November 1997)

A method for the solution of the two-electron problem in a strong magnetic field is presented that combines the well-known hyperspherical close-coupling and finite element methods and applied to helium in a magnetic field of up to 10^5 T, giving energy levels of low-lying S and P states up to a principal quantum number of $n=4$ as well as wavelengths of selected transitions. [S1050-2947(98)01205-0]

PACS number(s): 36.60.+i, 32.30.−r, 95.30.Ky

I. INTRODUCTION

Since the late 1960s evidence has been emerging that huge magnetic fields exist in the vicinity of compact cosmic objects such as neutron stars ($B\approx 10^7-10^9$ T) and white dwarf stars ($B\approx 10^2-10^5$ T). Those strong to very strong fields cause a drastic change in the atomic structure, and perturbation theory is no longer applicable. Thus atomic properties such as energy levels and wavelengths need to be recalculated from scratch. Due to the reduction of symmetry from spherical to cylindrical and due to the increase in the number of degrees of freedom advanced numerical methods are necessary.

Much work has already been done in calculating atomic energy values and oscillator strengths and as far as the hydrogen atom in a strong magnetic field is concerned numerically exact results have been produced for a wide range of states and magnetic field strengths [1]. Thus the problem of hydrogen in magnetic fields can be considered solved.

However, the situation for the helium atom and helium-like atoms in strong magnetic fields is by comparison quite different. So far the problem has mostly been treated on a Hartree-Fock level [2,3] and expansions in a complete basis set have only been applied recently [4]. In another recent development large-scale Monte Carlo calculations have been employed to obtain energy levels of He in a strong magnetic field [5]. In this paper we present a method that combines the well known hyperspherical close coupling [6–8] and finite element methods [9] to calculate atomic data for the two-electron problem in a strong magnetic field and give some of the results obtained for energies and wavelengths in the case of He, comparing our results to those in the literature.

It has been suggested already [10] that certain broad absorption features in the spectrum of the white dwarf GD229 should be attributed to neutral He at a magnetic field of about 65 000 T. Therefore the properties of the helium atom in strong magnetic fields are of great relevance.

*Present address: Theoretische Physik I, Fakultät für Physik und Astronomie, Ruhr-Universität Bochum, D-44780 Bochum, Germany.

The paper is organized as follows: In Sec. I we briefly review the Hamiltonian and discuss the symmetries inherent to the system. In Sec. II we describe the application of the hyperspherical close coupling approach to our problem, Sec. III deals with the numerical methods used and we then present, in Sec. IV, some results of our calculations for energies and wavelengths of a number of dipole transitions with and without magnetic field and compare these results with some already published ones. Finally in Sec. V we present our conclusions.

II. THE TWO-ELECTRON ATOM IN A STRONG MAGNETIC FIELD

A. The Hamiltonian

We consider a system consisting of two electrons and a nucleus of charge Ze in a homogeneous magnetic field B along the z axis. If we use Z-scaled atomic units, i.e., as energy unit $E_Z=Z^2$ Rydberg and as length unit a_{Bohr}/Z, and if we neglect the finite mass of the nucleus, the Hamiltonian reads

$$H=\sum_{i=1}^{2}\left[-\nabla_i^2-\frac{2}{|\boldsymbol{r}_i|}+\beta_Z^2(x_i^2+y_i^2)\right]+\frac{2}{Z|\boldsymbol{r}_1-\boldsymbol{r}_2|}+2\beta_Z[\boldsymbol{L}_z+g_e\boldsymbol{S}_z], \tag{1}$$

with $\beta_Z=B/(Z^2\times 4.7010\times 10^5\ \mathrm{T})$ and the g factor g_e of the electron. Note that the finite mass m_{nuc} of the nucleus can be taken into account in an approximate manner if the units are appropriately rescaled [11]. We also neglect spin-orbit coupling, as relativistic effects at the level of accuracy required for astrophysical applications are not considered to be important.

B. Symmetries of the Hamiltonian

The Hamiltonian (1) is invariant under rotation with respect to the z axis and inversion with respect to the origin, i.e., the parity operation. Therefore the good quantum numbers of the Hamiltonian are (i) the z component M of the total angular momentum $\boldsymbol{L}$, (ii) the parity P, (iii) the total spin S, (iv) its z component M_S. Thus the eigenstates of the Hamiltonian can be labeled by $|PMSM_S;\nu\rangle$. However, since we are concerned with the case of $\beta_Z \leqslant 0.05$ [12] in this paper, it is more convenient to label the states by the corresponding field-free states of helium. This correspondence is discussed in [2]. Therefore we label the states by $N^{(2S+1)}L_M$ in terms of the principal quantum number n, the total orbital angular momentum L, the magnetic quantum number M, and the total spin S.

III. THE HYPERSPHERICAL CLOSE-COUPLING APPROACH

A. The coordinates used

Instead of the radius vectors $\boldsymbol{r}_i$ we use the Jacobi coordinates

$$\boldsymbol{\xi}_1 = \frac{1}{\sqrt{2}}(\boldsymbol{r}_1 - \boldsymbol{r}_2) \tag{2}$$

and

$$\boldsymbol{\xi}_2 = \frac{1}{\sqrt{2}}(\boldsymbol{r}_1 + \boldsymbol{r}_2), \tag{3}$$

as in these coordinates the symmetry requirements of the Pauli principle are straightforward. Since they are related to the radius vectors by an orthogonal transformation, the diamagnetic part of the Hamiltonian, quadratic in β_Z, takes the same form in terms of the Jacobi vectors. We describe the system by three internal coordinates and three Eulerian angles α, β, and γ, that specify the orientation of the body fixed frame with respect to the laboratory frame. As internal coordinates, we choose the hyperradius

$$R = \sqrt{\xi_1^2 + \xi_2^2}, \tag{4}$$

the hyperangle

$$\phi = \arctan\left(\frac{\xi_2}{\xi_1}\right), \tag{5}$$

and the angle u between $\boldsymbol{\xi}_1$ and $\boldsymbol{\xi}_2$. The z' axis is chosen to be parallel to $\boldsymbol{\xi}_1$ and the y' axis perpendicular to $\boldsymbol{\xi}_1$ and $\boldsymbol{\xi}_2$. Thus both Jacobi vectors lie in the x'-z' plane.

B. The eigenfunctions of the symmetric top

We are going to expand our wave function in terms of the definite parity eigenfunctions of the symmetric top. They are defined by [13].

$$|PJMQ\rangle_\Omega = \frac{1}{\sqrt{2}}[|JMQ\rangle_\Omega + P(-1)^{J+Q}|JM-Q\rangle_\Omega], \quad Q>0,$$

$$|PJM0\rangle_\Omega = \frac{1}{2}[|JM0\rangle_\Omega + P(-1)^{J}|JM0\rangle_\Omega] \tag{6}$$

with

$$|JMK\rangle_\Omega = \sqrt{\frac{2J+1}{8\pi^2}} D_{MK}^{J*}(\alpha,\beta,\gamma), \tag{7}$$

where the coefficients of the representation of the rotation group are given by

$$D_{MM'}^{J}(\alpha,\beta,\gamma) = \langle JM|e^{-i\alpha L_z}e^{-i\beta L_y}e^{-i\gamma L_z}|JM'\rangle = e^{-iM\alpha}d_{MM'}^{J}(\beta)e^{-iM'\gamma}. \tag{8}$$

The non-negative quantum number Q designates the absolute value of the projection of the angular momentum onto the z' axis. The eigenfunctions for $P=1$ and $Q=0$ exist only for even J and the eigenfunctions for $P=-1$ and $Q=0$ exist only for odd J.

C. Transformation of the Hamiltonian

Except for the diamagnetic part of the Hamiltonian, the transformation of the Hamiltonian to Eulerian angles and the internal coordinates can be found in [8]. The diamagnetic term can be transformed by expressing it in terms of spherical harmonics in the laboratory frame and transforming to spherical harmonics in the body fixed frame [11].

The Hamiltonian is in terms of the internal coordinates R, ϕ, and u, the components of the total angular momentum J_i, $i=1,\ldots,3$ with respect to the body-fixed frame and the eigenfunctions of the symmetric top

$$H = -\left(\frac{\partial^2}{\partial R^2} + \frac{5}{R}\frac{\partial}{\partial R}\right) + \frac{1}{R^2}\left(-\frac{1}{\sin\phi\cos\phi}\frac{\partial^2}{\partial\phi^2}\sin\phi\cos\phi - 4 - \frac{1}{\sin^2\phi\cos^2\phi\sin u}\frac{\partial}{\partial u}\sin u\frac{\partial}{\partial u} + \frac{J_3^2}{\sin^2\phi\cos^2\phi\sin^2 u} - \frac{2J_3^2 - \boldsymbol{J}^2}{\cos^2\phi} + \frac{2iJ_2\frac{\partial}{\partial u} + 2\cot u J_1 J_3}{\cos^2\phi}\right) + \frac{C(\phi,u)}{R} + \beta_Z^2 R^2\left(\frac{2}{3} + \sqrt{\frac{8\pi^2}{5}}\sum_{q=0}^{2} p_q(\phi,u)|+20q\rangle_\Omega\right) + 2\beta_Z[\boldsymbol{L}_z + g_e\boldsymbol{S}_z], \tag{9}$$

where

$$C(\phi,u)=\frac{\sqrt{2}}{Z\cos\phi}-2\sqrt{2}\left(\frac{1}{\sqrt{1+\cos u\sin 2\phi}}+\frac{1}{\sqrt{1-\cos u\sin 2\phi}}\right),$$

$$p_0(\phi,u)=-\frac{2}{3}\cos^2\phi-\sin^2\phi\left(\cos^2 u-\frac{1}{3}\right),$$

$$p_1(\phi,u)=\frac{1}{\sqrt{3}}\sin^2\phi\sin 2u,$$

$$p_2(\phi,u)=-\frac{1}{\sqrt{3}}\sin^2\phi\sin^2 u. \tag{10}$$

By expanding the reduced wave function

$$\Phi(R,\phi,u,\Omega)=R^{5/2}\sin\phi\cos\phi\Psi, \tag{11}$$

in terms of the eigenfunctions of the symmetric top up to a maximum J value $J_{\max}$

$$\Phi=\sum_{J=|M|}^{J_{\max}}\sum_{Q}\Phi(R,\phi,u)_{J,Q}|PJMQ\rangle_{\Omega}|SM_S\rangle \tag{12}$$

and projecting onto the $|PJMQ\rangle_{\Omega}$ we obtain the following system of coupled partial differential equations:

$$\left[-\frac{\partial^2}{\partial R^2}+\frac{1}{R^2}\left(-\frac{1}{4}-\frac{\partial^2}{\partial\phi^2}-\frac{1}{\sin^2\phi\cos^2\phi\sin u}\frac{\partial}{\partial u}\sin u\frac{\partial}{\partial u}+\frac{Q^2}{\sin^2\phi\cos^2\phi\sin^2 u}-\frac{2Q^2-J(J+1)}{\cos^2\phi}\right)+\frac{C(\phi,u)}{R}\right]\Phi_{JQ}$$
$$+\frac{1}{R^2}\sum_{Q'}\frac{\langle PJMQ|2iJ_2|PJMQ'\rangle\partial/\partial u+\langle PJMQ|2J_1J_3|PJMQ'\rangle\cot u}{\cos^2\phi}\Phi_{JQ'}+\beta_Z^2R^2\sum_{J'Q'}\left(\frac{2}{3}\delta_{JJ'}\delta_{QQ'}\right.$$
$$\left.+\sqrt{\frac{8\pi^2}{5}}\sum_{k=0}^{2}\langle PJMQ|+20k|PJ'MQ'\rangle p_k(\phi,u)\right)\Phi_{J',Q'}+2\beta_Z[M+g_eM_S]\Phi_{JQ}=E\Phi_{JQ}. \tag{13}$$

D. Boundary conditions for the Φ_{JQ}

The boundary conditions for Φ_{JQ} have to be determined from the Pauli principle and the properties of the $|PJMQ\rangle_{\Omega}$. Exchanging the electrons results in $\boldsymbol{\xi}_1\to-\boldsymbol{\xi}_1$ but leaves $\boldsymbol{\xi}_2$ unchanged. In terms of the internal coordinates and the Eulerian angles this means that the hyperradius is unchanged while [13]

$$u\to\pi-u,$$
$$\alpha\to\alpha+\pi, \tag{14}$$
$$\beta\to\pi-\beta,$$
$$\gamma\to 2\pi-\gamma. \tag{15}$$

Using the definition of the $|PJMQ\rangle_{\Omega}$ and the properties of the $d^J_{MM'}(\beta)$ one arrives at the following symmetry requirement:

$$\Phi_{JQ}(\phi,\pi-u,R)=P(-1)^{S+Q}\Phi_{JQ}(\phi,u,R). \tag{16}$$

If the u interval is restricted to $[0,\pi/2]$, this leads to a condition for the derivative with respect to u at $u=\pi/2$. The boundary condition at $u=0$ is

$$\Phi_{JQ}(\phi,0,R)=0 \quad \text{for } Q>0 \tag{17}$$

because for $u=0$ the angle γ is undefined such that the coefficient of $|PJMQ\rangle_{\Omega}$ has to vanish for $Q>0$.

E. The adiabatic basis functions

The adiabatic basis functions are chosen to satisfy

$$\left[\frac{1}{R^2}\left(-\frac{\partial^2}{\partial\phi^2}-\frac{1}{\sin^2\phi\cos^2\phi\sin u}\frac{\partial}{\partial u}\sin u\frac{\partial}{\partial u}\right.\right.$$
$$\left.+\frac{Q^2}{\sin^2\phi\cos^2\phi\sin^2 u}-\frac{2Q^2-J(J+1)}{\cos^2\phi}\right)$$
$$\left.+\frac{C(\phi,u)}{R}\right]a_{JQ\lambda}(\phi,u,R)=U_{JQ\lambda}(R)a_{JQ\lambda}(\phi,u,R). \tag{18}$$

Since the hyperradius R is not affected by the exchange of the electrons the same boundary conditions as above are valid for the adiabatic basis functions.

F. The hyperradial equations

Expanding Φ in terms of the adiabatic basis functions

$$\Phi=\sum_{JQ\lambda} f_{JQ\lambda}(R)a_{JQ\lambda}(\phi,u,R)|PJMQ\rangle_\Omega|SM_S\rangle, \tag{19}$$

we obtain the following system of differential equations in R

$$\left[-\frac{\partial^2}{\partial R^2}+U_{JQ\lambda}(R)-\frac{1}{4R^2}+2\beta_Z[M+g_e M_S]+\frac{2}{3}\beta_Z^2R^2\right]f_{JQ\lambda}(R)-\sum_\mu\left[2\left\langle a_{JQ\lambda}\left|\frac{\partial}{\partial R}\right|a_{JQ'\mu}\right\rangle(R)\frac{\partial f_{JQ\mu}(R)}{\partial R}\right.$$
$$\left.+\left\langle a_{JQ\lambda}\left|\frac{\partial^2}{\partial R^2}\right|a_{JQ'\mu}\right\rangle(R)f_{JQ\mu}(R)\right]+\sum_{Q'\mu}\frac{1}{R^2}\left[\langle PJMQ|2iJ_2|PJMQ'\rangle\left\langle a_{JQ\lambda}\left|\frac{1}{\cos^2\phi}\frac{\partial}{\partial u}\right|a_{JQ'\mu}\right\rangle(R)\right.$$
$$\left.+\langle PJMQ|2J_1J_3|PJMQ'\rangle\left\langle a_{JQ\lambda}\left|\frac{\cot u}{\cos^2\phi}\right|a_{JQ'\mu}\right\rangle(R)f_{JQ'\mu}(R)\right]$$
$$+\beta_Z^2R^2\sum_{J'Q'\mu}\sum_{k=0}^{2}\sqrt{\frac{8\pi^2}{5}}\langle PJMQ|+20k|PJ'MQ'\rangle\langle a_{JQ\lambda}|p_k(\phi,u)|a_{J'Q'\mu}\rangle(R)f_{J'Q'\mu}(R)=Ef_{JQ\lambda}(R). \tag{20}$$

For the evaluation of the various matrix elements between the $|PJMQ\rangle_\Omega$ see Appendix A.

IV. NUMERICAL METHODS USED

We employed the method of finite elements for the determination of the adiabatic basis functions as well as for the solution of the hyperradial differential equations. This method has already been applied to a number of problems in atomic physics [14,15,9,11]

A. Determination of the adiabatic basis functions

The area $[0,\pi/2]\times[0,\pi/2]$ is subdivided into $n_\phi\times n_u$ rectangular elements. On each element the adiabatic basis function a is expanded in terms of biquintic splines. The expansion coefficients are the 36 values of the adiabatic basis function and its partial derivatives of up to second order in ϕ and u at the 4 corners of the element.

Application of the variational principle leads to a generalized symmetric eigenvalue problem

$$Hx=\lambda Ux \tag{21}$$

that is solved by subspace iteration [16].

B. Solution of the hyperradial equations using FEM

The interval $[0,R_{\max}]$ is subdivided into n_r elements $[R_{i-1},R_i]$ according to

$$R_i=\left(\frac{i}{n_r}\right)^2R_{\max}. \tag{22}$$

The adiabatic basis functions are calculated on a grid consisting of the Gauss-Legendre integration points of order n_g with respect to the above elements. In addition the adiabatic basis functions are also calculated on two grids shifted by h and $-h$, using the prescription

$$\frac{\partial f(R)}{\partial R}=\frac{f(R+h)-f(R-h)}{2h}+O(h^3) \tag{23}$$

to obtain the derivative of the adiabatic basis functions.

To apply the method of finite elements the variational principle is employed to our ansatz (19) yielding upon partial integration a symmetric generalized eigenvalue problem that is also treated via inverse iteration.

TABLE I. Comparison of energies for low-lying S and P states of He with those of Accad *et al.*

State	E/E_Z	$\Delta E/E_Z$
$1\,^1S$	−1.451 8580	4.2×10^{-6}
$2\,^1S$	−1.072 969	1.8×10^{-5}
$3\,^1S$	−1.030 601	3.5×10^{-5}
$4\,^1S$	−1.0153	1.2×10^{-3}
$2\,^1P$	−1.0610	9.2×10^{-4}
$2\,^3S$	−1.087 6149	2.1×10^{-7}
$3\,^3S$	−1.034 3412	3.3×10^{-6}
$4\,^3S$	−1.017 35	9.1×10^{-4}
$5\,^3S$	−1.0026	8.7×10^{-3}
$2\,^3P$	−1.0656	9.8×10^{-4}

TABLE II. Oscillator strengths for selected dipole transitions between low-lying S and P states.

Transition	This work	Tang *et al.* [10]
$2\,^1P_0\rightarrow1\,^1S_0$	0.267	0.276
$3\,^1P_0\rightarrow2\,^1S_0$	0.144	0.149
$2\,^1P_0\rightarrow2\,^1S_0$	0.423	0.377
$3\,^1P_0\rightarrow1\,^1S_0$	0.070	0.074

TABLE III. Energies in units of E_Z of singlet S states for $M=0$.

β_Z	$1\,^1S$	$2\,^1S$	$3\,^1S$	$4\,^1S$
0.000	−1.451 8580	−1.072 9690	−1.030 6007	−1.015 2540
0.002	−1.451 8325	−1.072 6272	−1.028 8570	−1.011 1947
0.004	−1.451 7562	−1.071 6199	−1.024 2392	−1.000 8726
0.006	−1.451 6289	−1.069 9934	−1.017 6783	−0.987 4711
0.008	−1.451 4509	−1.067 8065	−1.009 7779	−0.972 4952
0.010	−1.451 2222	−1.065 1190	−1.000 8983	−0.956 4792
0.012	−1.450 9429	−1.061 9856	−0.991 2658	−0.939 6979
0.014	−1.450 6131	−1.058 4537	−0.981 0314	−0.922 3212
0.016	−1.450 2331	−1.054 5644	−0.970 3012	−0.904 4633
0.018	−1.449 8031	−1.050 3524	−0.959 1527	−0.886 2057
0.020	−1.449 3232	−1.045 8473	−0.947 6446	−0.867 6088
0.030	−1.446 1851	−1.019 7087	−0.886 0420	−0.770 8767
0.040	−1.441 8447	−0.988 9480	−0.819 7168	−0.669 9162
0.050	−1.436 3474	−0.954 7902	−0.750 2266	−0.566 2224

TABLE V. Energies in units of E_Z of triplet S states for $M=0$.

β_Z	$2\,^3S$	$3\,^3S$	$4\,^3S$
0.000	−1.087 6149	−1.034 3412	−1.017 3498
0.002	−1.087 3710	−1.032 9256	−1.013 5688
0.004	−1.086 6474	−1.029 0867	−1.004 0890
0.006	−1.085 4659	−1.023 4986	−0.991 7632
0.008	−1.083 8566	−1.016 6489	−0.977 8820
0.010	−1.081 8528	−1.008 8511	−0.962 9496
0.012	−1.079 4872	−1.000 3111	−0.947 2355
0.014	−1.076 7903	−0.991 1698	−0.930 9065
0.016	−1.073 7897	−0.981 5281	−0.914 0749
0.018	−1.070 5097	−0.971 4602	−0.896 8204
0.020	−1.066 9719	−0.961 0230	−0.879 2023
0.030	−1.046 0047	−0.904 5799	−0.786 9664
0.040	−1.020 6728	−0.843 0189	−0.689 7985
0.050	−0.991 9694	−0.777 8476	−0.589 1934

V. RESULTS AND DISCUSSION

Using the method explained above the energies of both triplet and singlet S and P states of He up to a principal quantum number of $n=4$ have been calculated for $\beta_Z \leqslant 0.1$. Due to computational requirements of a fully coupled calculation, we have so far restricted the expansion to one value of the total orbital angular momentum. Thus we have been able to obtain the wavelengths of quite a number of dipole transitions between S and P states. In addition we have calculated the dipole matrix elements and thus the oscillator strengths for a number of transitions at zero field using a formalism detailed in Appendix B

A. Results without magnetic field

1. Energies

As a test of our method we consider the eigenstates of nonrelativistic helium without magnetic field, for which very accurate results are available in the literature [17–19]. In Table I we give our results for a number of states and their deviation from the results of [17]. The agreement of our energies with the reference values is good to very good for S states, while fair for P states.

2. Oscillator strengths

As a further test of our method, which is also sensitive to the quality of the wave functions, we compare in Table II our results obtained for the zero-field oscillator strengths, for a few transitions with those obtained by [20]. The agreement is quite satisfactory except for $2\,^1P_0 \rightarrow 2\,^1S_0$, due to the small energy difference, its wavelength being very large and thus unimportant for astrophysical applications.

B. Results with magnetic field

1. Energies

In Tables III to VI we give the results obtained for the energies of the singlet and triplet S and P states for $\beta_Z \leqslant 0.05$ and principal quantum number $n \leqslant 4$. Since the spin only introduces a trivial linear energy dependence, we only con-

TABLE IV. Energies (as in Table III) of singlet P states for $M=0$.

β_Z	$2\,^1P$	$3\,^1P$	$4\,^1P$
0.000	−1.061 0026	−1.026 7741	−1.013 1498
0.002	−1.060 7966	−1.025 6291	−1.010 6442
0.004	−1.060 1888	−1.022 5454	−1.003 8476
0.006	−1.059 2057	−1.018 1159	−0.994 4838
0.008	−1.057 8819	−1.012 7566	−0.983 8601
0.010	−1.056 2534	−1.006 7212	−0.972 4939
0.012	−1.054 3534	−1.000 1709	−0.960 6010
0.014	−1.052 2115	−0.993 2132	−0.948 3046
0.016	−1.049 8530	−0.985 9234	−0.935 6849
0.018	−1.047 2995	−0.978 3562	−0.922 7979
0.020	−1.044 5695	−0.970 5526	−0.909 6847
0.030	−1.028 7533	−0.928 8942	−0.841 6077
0.040	−1.010 1713	−0.884 1787	−0.770 6274
0.050	−0.989 5395	−0.837 3776	−0.697 6668

TABLE VI. Energies (as in Table III) of triplet P states for $M=0$.

β_Z	$2\,^3P$	$3\,^3P$	$4\,^3P$
0.000	−1.065 5938	−1.028 1475	−1.014 0865
0.002	−1.065 4235	−1.027 1175	−1.011 6499
0.004	−1.064 9194	−1.024 3209	−1.005 1073
0.006	−1.064 1004	−1.020 2657	−0.996 1622
0.008	−1.062 9920	−1.015 3249	−0.986 0204
0.010	−1.061 6214	−1.009 7349	−0.975 1585
0.012	−1.060 0148	−1.003 6492	−0.963 7858
0.014	−1.058 1959	−0.997 1716	−0.952 0227
0.016	−1.056 1858	−0.990 3755	−0.939 9470
0.018	−1.054 0025	−0.983 3141	−0.927 6120
0.020	−1.051 6620	−0.976 0275	−0.915 0558
0.030	−1.038 0161	−0.937 0880	−0.849 7693
0.040	−1.021 8745	−0.895 2337	−0.781 5296
0.050	−1.003 8713	−0.851 3485	−0.711 2809

TABLE VII. Energies of He in units of E_Z at $\beta_Z=0.025$ determined by different methods.

State	This work	Scrinzi	Larsen
$1\,^1S$	−1.4479	−1.4477	−1.4468
$2\,^1P_0$	−1.0365	−1.0403	−1.0402

sider $M_S=0$ here. The chosen grid of β_Z values is sufficiently fine to interpolate for values of β_Z in between. The parameters of the calculation were $R_{\max}=64$, $n_\phi=20$, $n_u=10$, $n_r=16$, $n_g=16$, and $n_{\text{adia}}=25$ adiabatic basis functions were used in each channel.

In Table VII we compare our results for $\beta_Z=0.025$ with the variational calculations by Scrinzi [4] and Larsen [21]. The agreement obtained is good for S while fair for P states. The ground-state energy obtained by our method is lower, while the opposite is true for 2^1P, which can be attributed to the fact that angular momentum mixing, expected to be more important for $J>0$ states, was included in their calculations.

In Table VIII we compare our energies obtained for the ground state 1^1 and for triplet states with $n\leqslant 3$ for $\beta_Z=0.01$, 0.03, and 0.05 with the spin-unrestricted Hartree-Fock (UHF) results from [3]. Our results for the ground state are quite a bit lower, which is due to the absence of correlation in HF calculations. For the triplet states, where correlations are less important, the agreement is good for $n=2$ while there are some discrepancies at the larger values of β_Z for $n=3$, especially for the S state. This can be explained by the fact that we did not include a coupling between S and D states, which is well known [1] to be important in the case of hydrogen in a strong magnetic field, where the $3s$ and $3d_0$ states are mixed even in the limit $\beta_Z\rightarrow 0$. Thus our calculation for the $3\,^3S$ state is reliable only for β_Z small enough for the energy difference between the $3\,^3D$ and $3\,^3P$ states to dominate over the coupling between them due to the diamagnetic part of the Hamiltonian.

In Table IX we compare our energies at $\beta_Z=0$ and 0.01 for a number of states with those given in [5], which were obtained using the released-phase quantum Monte Carlo formalism. The agreement at $\beta_Z=0$ is quite good, while their energies are, especially for the higher excited states, somewhat lower at $\beta_Z=0.01$.

Note that the energies of triplet states obtained in both the UHF and released-phase quantum Monte Carlo (RPQMC) calculations are for $M_S=-1$, which means they have to be corrected by a linear term.

2. Wavelengths

In Figs. 1 and 2 the wavelengths obtained with our method for selected electromagnetic dipole transitions are shown as a function of β_Z for $\beta_Z\leqslant 0.05$. From the comparison with literature values at $\beta_Z=0$ and with variational and Monte Carlo calculations for $\beta_Z>0$ above we estimate our wavelengths to have an accuracy of a few percent for $\beta_Z\leqslant 0.025$. A number of the transitions shown exhibit maxima in the wavelength, which, as is well known from the study of hydrogen in the atmosphere of magnetic white dwarfs [22], can lead to prominent absorption features.

Maxima appear only in those transitions in which the higher state has a magnetic quantum number $M=-1$, which can be easily understood since the energy of the P state will show a linear behavior for small β_Z, while the influence of the diamagnetic term takes over for moderately large β_Z, having the opposite sign. The lower state will have a quadratic behavior at small values of β_Z, but no linear term. Those maxima are quite pronounced for the singlet case, while rather weak in comparison for the triplet case.

VI. CONCLUSIONS

The combination of the hyperspherical close coupling and finite element method has been shown to provide energy values and wavelengths of sufficient accuracy to be used as input into model calculations for atmospheres of magnetic white dwarfs. From the comparison with competing methods like UHF and RPQMC it seems that our method is superior for singlet states with a high degree of correlation while the UHF results are of comparable quality or better for triplet states especially for $n\geqslant 3$.

We plan to extend our calculations to include angular momentum mixing, which will allow us to obtain accurate results also for larger β_Z values and to obtain oscillator strengths for nonzero fields, which are an essential input for any model calculation of stellar spectra.

ACKNOWLEDGMENTS

The authors acknowledge support from the South African Foundation for Research Development (FRD) and the Deutsche Forschungsgemeinschaft (DFG).

APPENDIX A: VARIOUS MATRIX ELEMENTS

Most of the matrix elements involving the $|PJMQ\rangle$ appearing in Eq. (20) can be evaluated by applying well-known

TABLE VIII. Comparison of energies in units of E_Z obtained for He at $\beta_Z=0.01$, 0.03, and 0.05 with the results of UHF calculations by Jones *et al.*

β_Z	0.01		0.03		0.05	
State	This work	Jones *et al.*	This work	Jones *et al.*	This work	Jones *et al.*
$1\,^1S$	−1.451 2222	−1.4302	−1.446 1851	−1.4252	−1.436 3474	−1.4155
$2\,^3S$	−1.081 8528	−1.0815	−1.046 0047	−1.0491	−0.991 9694	−1.0056
$3\,^3S$	−1.008 8511	−1.0190	−0.904 5799	−0.976 35	−0.777 8476	−0.9308
$2\,^3P_0$	−1.061 6214	−1.0618	−1.038 0161	−1.0399	−1.003 8713	−1.0098
$3\,^3P_0$	−1.009 7349	−1.0147	−0.937 0880	−0.9753	−0.851 3485	−0.9351

TABLE IX. Comparison of energies in units of E_Z obtained for He at $\beta_Z=0.0$ and 0.01 with the results of released-phase quantum Monte Carlo calculations by Jones *et al.*

β_Z	0.0		0.01	
State	This work	Jones *et al.*	This work	Jones *et al.*
$2\,^3S$	−1.087 6149	−1.0876(3)	−1.081 8528	−1.0819(2)
$3\,^3S$	−1.034 3412	−1.0344(1)	−1.008 8511	−1.0205(1)
$4\,^3S$	−1.017 3498	−1.0183(1)	−0.962 9496	−0.9944(5)
$2\,^3P_0$	−1.065 5938	−1.0670(4)	−1.061 6214	−1.0625(3)
$3\,^3P_0$	−1.028 1475	−1.0291(1)	−1.009 7349	−1.0150(2)
$4\,^3P_0$	−1.014 0865	−1.0162(1)	−0.975 1585	−0.9889(7)

relations for the body-fixed components of the angular momentum.

The matrix elements of the $|+20q\rangle$ that appear in the diamagnetic part of the hyperradial equations can be found by using the following relation [23]:

$$\int d\Omega D^{j_3 *}_{m_3 m_3'} D^{j_2}_{m_2 m_2'} D^{j_1}_{m_1 m_1'} = \frac{8\pi^2}{2j_3+1}\,\delta_{m_1+m_2,m_3}\delta_{m_1'+m_2',m_3'} \times \begin{pmatrix} j_1 & j_2 & \big| & j_3 \\ m_1 & m_2 & \big| & m_1+m_2 \end{pmatrix} \times \begin{pmatrix} j_1 & j_2 & \big| & j_3 \\ m_1' & m_2' & \big| & m_1'+m_2' \end{pmatrix} \quad \text{(A1)}$$

for the integral over the product of three representation coefficients of the rotation group and applying Eq. (4.19) from [23]

$$d^J_{-M,-M'}(\beta) = (-1)^{M-M'} d^J_{M,M'}(\beta). \quad \text{(A2)}$$

The final result for the different matrix elements needed is

$$\langle PJMQ|2iJ_2|PJMQ'\rangle = \delta_{J,J'}\delta_{Q,Q'-1}\sqrt{(J+Q+1)(J-Q)}[1+(\sqrt{2}-1)\delta_{Q,0}] - \delta_{J,J'}\delta_{Q,Q'+1}\sqrt{(J-Q+1)(J+Q)}[1+(\sqrt{2}-1)\delta_{Q,1}], \quad \text{(A3)}$$

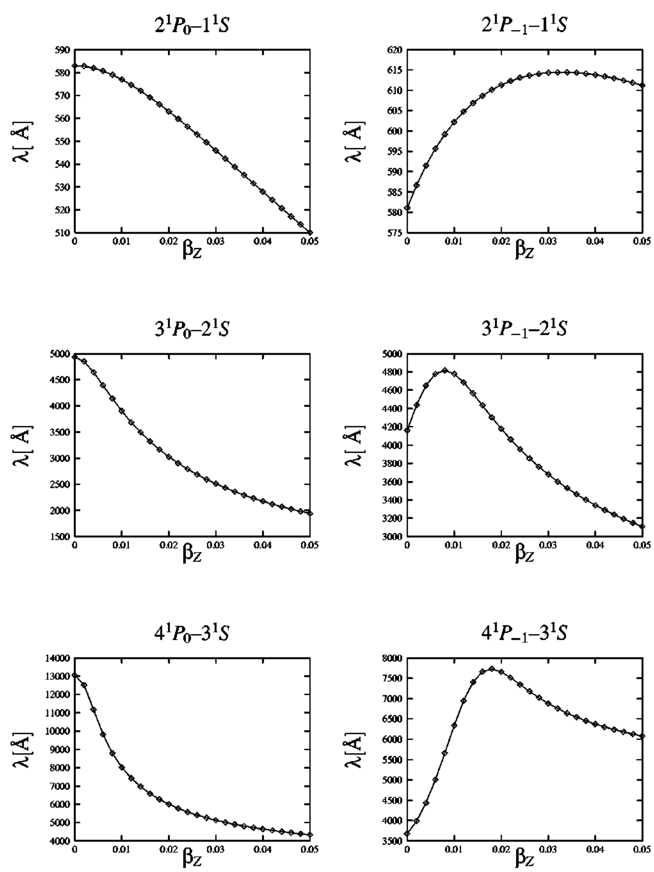

FIG. 1. Wavelengths of selected dipole transitions between singlet S and P states.

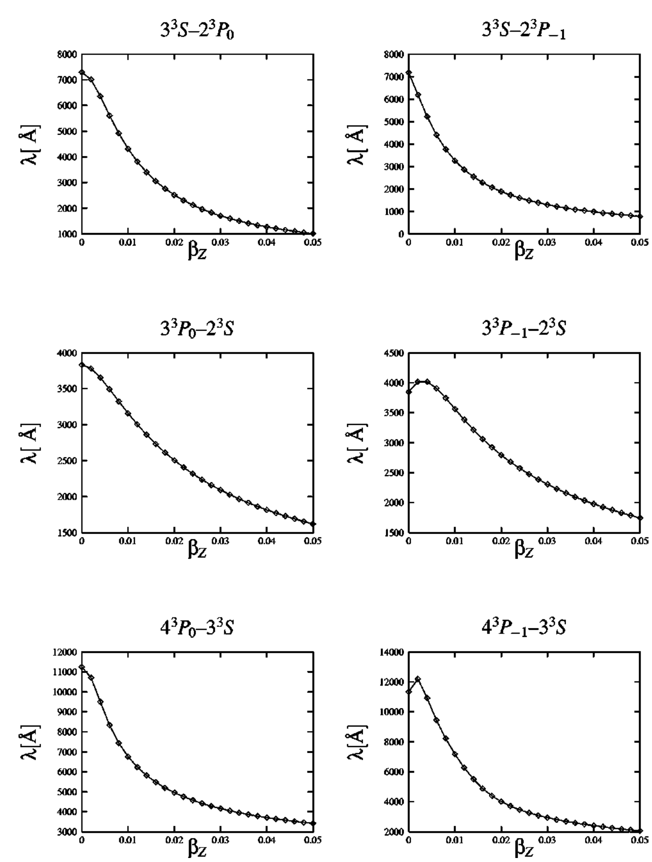

FIG. 2. Wavelengths of selected dipole transitions between triplet S and P states.

$$\langle PJMQ|2J_1J_3|PJMQ'\rangle=\delta_{J,J'}\delta_{Q,Q'-1}\sqrt{(J+Q+1)(J-Q)}[1+(\sqrt{2}-1)\delta_{Q,0}](Q+1)+\delta_{J,J'}\delta_{Q,Q'+1}\sqrt{(J-Q+1)(J+Q)}[1+(\sqrt{2}-1)\delta_{Q,1}](Q-1), \tag{A4}$$

$$\sqrt{\frac{8\pi^2}{5}}\langle PJMQ|+,20q|PJ'MQ'\rangle=\frac{1}{\sqrt{2(1+\delta_{Q'0})(1+\delta_{q0})(1+\delta_{Q0})}}\sqrt{\frac{2J'+1}{2J+1}}\begin{pmatrix}J' & 2 & J\\ M & 0 & M\end{pmatrix}\times\left[\begin{pmatrix}J' & 2 & J\\ Q' & q & Q\end{pmatrix}+P(-1)^{J+Q}\begin{pmatrix}J' & 2 & J\\ Q' & q & -Q\end{pmatrix}+(-1)^{q}\begin{pmatrix}J' & 2 & J\\ Q' & -q & Q\end{pmatrix}+P(-1)^{J'+Q'}\begin{pmatrix}J' & 2 & J\\ -Q' & q & Q\end{pmatrix}\right]. \tag{A5}$$

APPENDIX B: DETERMINATION OF DIPOLE MATRIX ELEMENTS

The dipole matrix elements for a $\Delta M=q$ transition from the initial state

$$|i\rangle=|P_iM_iSM_S;\nu_i\rangle.$$

to the final state

$$|f\rangle=|P_fM_fSM_S;\nu_f\rangle.$$

are defined via

$$d_{fi}^{(q)}=\left\langle f\left|\sum_{i=1}^{2}r_i^{(q)}\right|i\right\rangle \tag{B1}$$

with

$$r_i^{(q)}=\sqrt{\frac{4\pi}{3}}r_iY_{1q}(\hat{\boldsymbol{r}}_i). \tag{B2}$$

In terms of the Jacobi coordinates used the dipole matrix elements take the simpler form

$$d_{fi}^{(q)}=\langle f|R^{(q)}|i\rangle \tag{B3}$$

with

$$R^{(q)}=\sqrt{\frac{8\pi}{3}}\xi_2Y_{1q}(\hat{\boldsymbol{\xi}}_2). \tag{B4}$$

The transformation to internal coordinates and Eulerian angles [11] yields

$$R^{(q)}=\sqrt{\frac{8\pi^2}{3}}(\sqrt{2}R\sin\phi\cos u|-11q0\rangle_\Omega-\sqrt{2}R\sin\phi\sin u|-11q1\rangle_\Omega). \tag{B5}$$

Expanding the reduced wave functions Φ_f and Φ_i for the final and initial states in terms of the definite parity eigenfunctions of the symmetric top $|PJMQ\rangle_\Omega$ and of the adiabatic eigenfunctions $a_{JQ\lambda}(\phi,u,R)$,

$$\Phi_f=\sum_{J_f=|M_f|}^{J_{\max}}\sum_{Q_f}\sum_{\lambda}f_\lambda^{J_fQ_f}(R)a_{fJ_fQ_f\lambda}(\phi,u,R)|P_fJ_fM_fQ_f\rangle, \tag{B6}$$

$$\Phi_i=\sum_{J_i=|M_i|}^{J_{\max}}\sum_{Q_i}\sum_{\mu}g_\mu^{J_iQ_i}(R)a_{iJ_iQ_i\mu}(\phi,u,R)|P_iJ_iM_iQ_i\rangle \tag{B7}$$

the dipole matrix elements take the final form

$$d_{fi}^{(q)}=\sqrt{\frac{8\pi^2}{3}}\sum_{J_f=|M_f|}^{J_{\max}}\sum_{Q_f}\sum_{J_i=|M_i|}^{J_{\max}}\sum_{Q_i}\sum_{\lambda\mu}[\sqrt{2}\langle P_fJ_fM_fQ_f|-11q0|P_iJ_iM_iQ_i\rangle\langle f_\lambda^{J_fQ_f}|Rd_{\lambda\mu}^{J_fQ_fJ_iQ_i}(R)|g_\mu^{J_iQ_i}\rangle_R]-[\sqrt{2}\langle P_fJ_fM_fQ_f|-11q1|P_iJ_iM_iQ_i\rangle\langle f_\lambda^{J_fQ_f}|Re_{\lambda\mu}^{J_fQ_fJ_iQ_i}(R)|g_\mu^{J_iQ_i}\rangle_R] \tag{B8}$$

with

$$d_{\lambda\mu}^{J_fQ_fJ_iQ_i}(R)=\langle a_{fJ_fQ_f\lambda}|\sin\phi\cos u|a_{iJ_iQ_i\mu}\rangle_{\phi,u} \tag{B9}$$

and

$$e_{\lambda\mu}^{J_fQ_fJ_iQ_i}(R)=\langle a_{fJ_fQ_f\lambda}|\sin\phi\sin u|a_{iJ_iQ_i\mu}\rangle_{\phi,u}. \tag{B10}$$

The matrix elements of $|-,1qQ\rangle_\Omega$ between the $|PJMQ\rangle_\Omega$ can be evaluated using similar methods as in Appendix A yielding

$$\sqrt{\frac{8\pi^2}{3}}\langle P_fJ_fM_fQ_f|-,1qQ|P_iJ_iM_iQ_i\rangle=\frac{\delta_{P_fP_i,-1}}{\sqrt{2(1+\delta_{Q_f0})(1+\delta_{q0})(1+\delta_{Q0})}}\sqrt{\frac{2J_i+1}{2J_f+1}}\left(\begin{array}{cc|c} J_i & 1 & J_f \\ M_i & q & M_f \end{array}\right)\left[\left(\begin{array}{cc|c} J_i & 1 & J_f \\ Q_i & Q & Q_f \end{array}\right)+P_f(-1)^{J_f+Q_f}\left(\begin{array}{cc|c} J_i & 1 & J \\ Q_i & Q & -Q_f \end{array}\right)+(-1)^Q\left(\begin{array}{cc|c} J_i & 1 & J \\ Q_i & -Q & Q_f \end{array}\right)+P_i(-1)^{J_i+Q_i}\left(\begin{array}{cc|c} J_i & 1 & J_f \\ -Q_i & Q & Q_f \end{array}\right)\right]. \tag{B11}$$

For the dipole transition we thus recover the usual selection rules

$$P_fP_i=-1 \tag{B12}$$

and

$$M_f=M_i+q. \tag{B13}$$

[1] H. Ruder, G. Wunner, H. Herold, and F. Geyer, *Atoms in Strong Magnetic Fields* (Springer-Verlag, Berlin, 1994).

[2] G. Thurner, H. Körbel, M. Braun, H. Herold, H. Ruder, and G. Wunner, J. Phys. B **26**, 4719 (1993).

[3] M. D. Jones, G. Ortiz, and D. M. Ceperley, Phys. Rev. A **54**, 219 (1996).

[4] A. Scrinzi, J. Phys. B **29**, 6055 (1996).

[5] M. D. Jones, G. Ortiz, and D. M. Ceperley, Phys. Rev. E **55**, 6202 (1997).

[6] J. Tang, S. Watanabe, and M. Matsuzawa, Phys. Rev. A **46**, 2437 (1992).

[7] J. Tang, S. Watanabe, and M. Matsuzawa, Phys. Rev. Lett. **69**, 1633 (1992).

[8] Y. Zhou and C. D. Lin, J. Phys. B **27**, 5065 (1997).

[9] M. Braun, W. Schweizer, and H. Herold, Phys. Rev. A **48**, 1916 (1993).

[10] G. D. Schmidt and W. B. Latter, Astrophys. J. **350**, 758 (1990).

[11] M. Braun, Ph.D. thesis, University of Tübingen, Germany, 1993 (unpublished).

[12] The white dwarf star with the strongest observed polar magnetic field, $10^5T\approx\beta_Z=0.05$ is the DA white dwarf PG 1031 +234 (see also [1] Chap. 7).

[13] H. Ruder, Ph.D. thesis, University of Erlangen-Nürnberg, Germany, 1967 (unpublished).

[14] F. S. Levin and J. Shertzer, Phys. Rev. A **32**, 3285 (1985).

[15] J. Shertzer, L. R. Ram-Mohan, and D. Dossa, Phys. Rev. A **40**, 4777 (1989).

[16] K. J. Bathe and E. L. Wilson, *Numerical Methods in Finite Element Analysis* (Prentice-Hall, Englewood Cliffs, NJ, 1976).

[17] Y. Accad, C. L. Pekeris, and B. Schiff, Phys. Rev. A **4**, 516 (1971).

[18] G. W. F. Drake, Nucl. Instrum. Methods Phys. Res. B **31**, 7 (1988).

[19] G. W. F. Drake, in *Relativistic, Quantum Electrodynamics and Weak Interaction Effects in Atoms*, AIP Conf. Proc. No. 189, edited by W. H. Johnson *et al.* (American Institute of Physics, New York, 1989), p. 146.

[20] J. Tang, S. Watanabe, and M. Matsuzawa, Phys. Rev. A **46**, 3758 (1992).

[21] D. M. Larsen, J. Phys. B **20**, 5217 (1979).

[22] P. Faßbinder and W. Schweizer, Astron. Astrophys. **314**, 700 (1996).

[23] M. W. Rose, *Elementary Theory of Angular Momentum* (Wiley and Sons, New York, 1957).